Effectiveness of dust dispersion in the 20-L Siwek chamber

Omotayo Kalejaiye [a], Paul R. Amyotte [a], Michael J. Pegg [a,*], Kenneth L. Cashdollar [b]

[a] Department of Process Engineering and Applied Science, Dalhousie University, 1360 Barrington St., Halifax, Nova Scotia, Canada B3J 2X4
[b] Pittsburgh Research Laboratory, National Institute for Occupational Safety and Health, Pittsburgh, PA 15236, USA

A B S T R A C T

The Siwek 20-L chamber is widely used throughout the world to evaluate the explosibility of dusts. This research evaluated the quality of dust dispersion in the Siwek 20-L chamber using Pittsburgh coal, Gilsonite, and purple K dusts. A Pittsburgh Research Laboratory (PRL) optical dust probe was used to measure optical transmittance through the dust cloud at various locations within the chamber. A total of 540 tests were performed, with triplicate tests at five nominal dust concentrations and six locations. The two standard dispersion nozzles (rebound and perforated annular nozzle) were compared. The transmissions corresponding to the normal ignition delay period were used to: (a) determine variations in spatial uniformity of dispersion obtained with both nozzles; (b) make comparisons between the experimental transmission data and those calculated from theory for the three dusts; and (c) make comparisons with transmission data measured in the PRL 20-L and Fike 1-m^3 dust explosion chambers.

The uniformity of dispersion for the three dusts was similar with both nozzles, despite the differences in nozzle geometry and mode of operation. Transmission data of the three dusts were all significantly lower than those calculated from theory. This was discovered to be, in part, due to significant reduction in particle size that occurred during dispersion. By measuring particle sizes before and after dispersion, values of 60%, 50%, and 20% reduction in particle size (based on the surface-weighted mean diameter) were obtained for Pittsburgh coal, Gilsonite, and purple K, respectively. Transmission data from the PRL 20-L, Fike 1-m^3 and the Siwek 20-L chambers indicated comparable results in terms of uniformity of dispersion. However, transmission data from the Siwek 20-L chamber were significantly lower than those of the PRL and Fike chambers. Again, this was attributed, in part, to the significant reduction in particle size that occurred during dispersion in the Siwek chamber. The design of the outlet (dispersion) valve of the Siwek 20-L apparatus charge vessel was largely responsible for the particle break-up. The contribution to particle break-up by the dispersion nozzles and the high level of turbulence in the chamber were found to be minimal. This is a significant finding in that the dust particle size tested for explosibility in the Siwek chamber is considerably smaller than the original dust sample.

1. Introduction

The hazards associated with combustible dusts have been recognized for at least the past 200 years. There are five requirements for a dust explosion. The requirements for a fire are a fuel (combustible dust), an oxidant (usually oxygen in air), and an ignition source. The two additional requirements for an explosion are that the dust particles must be dispersed in air at the time of ignition and that there must be some degree of confinement.

The explosibility characteristics of dusts can be broadly classified into two categories. The first group describes the likelihood of a dust explosion occurring and this includes the minimum explosible concentration (MEC), the minimum ignition energy (MIE), the limiting oxygen concentration (LOC), and the minimum autoignition temperature (MAIT). The second group describes the severity of a dust explosion when it occurs and this includes the maximum explosion pressure (P_{max}) and the maximum rate of pressure rise ($[dP/dt]_{max}$). Another important quantity is the deflagration index or volume-normalized maximum rate of pressure rise. [$K_{St} = (dp/dt)_{max} \cdot V^{1/3}$] where V is the volume of the test chamber in m^3. Thus, K_{St} (in bar·m/s) is the maximum rate of pressure rise that would be obtained directly from a standard 1-m^3 test vessel. Combustible dusts are classified by their K_{St} values in increasing order of explosion violence as follows (Bartknecht, 1989): $0 < K_{St} \leq 200$ corresponds to St 1 dust explosion class; $200 < K_{St} \leq 300$ for St 2 dust explosion class; and $K_{St} > 300$ for St 3 dust explosion class. Furthermore, the K_{St} value of a combustible dust is an important factor that is considered in the determination of relief areas for venting, as specified in NFPA 68

* Corresponding author. Tel.: +1 902 494 3252; fax: +1 902 420 7639.
E-mail address: michael.pegg@dal.ca (M.J. Pegg).

(2002). Extensive discussion of these parameters has been given in the textbooks by Bartknecht (1989) and Eckhoff (1997).

The general procedure for the determination of explosibility characteristics of dusts is to disperse a known mass of the dust into the test chamber with a blast of air. For every test, the nominal dust concentration is determined by dividing the mass of dust dispersed by the fixed volume of the chamber. This approach is based on the assumption that the dust cloud formed is uniform (*i.e.* no variation in local dust concentration throughout the chamber volume). However, this is an ideal case, which may be difficult, or perhaps impossible, to achieve in reality. Clearly, the degree of dust cloud uniformity in test chambers can affect the accuracy of the results obtained, particularly the MEC data. Eggleston and Pryor (1967) showed that the degree of dust cloud uniformity in the 1.2-L Hartmann tube deviates significantly from the ideal case. Thus, inaccurate MEC values are obtained from the Hartmann test vessel.

Recognizing the errors that can be introduced into MEC data by highly non-uniform dust clouds in test chambers, the ASTM International standard test method E1515 (ASTM, 2005b) for the determination of minimum explosible concentrations of combustible dusts stipulates that the test apparatus must be capable of producing a fairly uniform dust cloud of the material. Among the available test apparatus that have been considered as suitable for dust explosibility tests by the ASTM is the Siwek 20-L chamber (Siwek, 1977) manufactured by Adolf Kühner AG, Birsfelden, Switzerland. For this apparatus, two different nozzles are available for dust dispersion, namely the rebound nozzle and the perforated annular nozzle. The dust cloud formed in this chamber is assumed to be fairly uniform, but this has never been documented quantitatively.

Therefore, the objectives of the present study (Kalejaiye, 2001) were to: (i) determine the variations in spatial uniformity of the dust cloud formed in the Siwek 20-L chamber using the rebound nozzle and the perforated annular nozzle; (ii) assess the effectiveness of dust dispersion in the Siwek 20-L chamber, in comparison to the Pittsburgh Research Laboratory (PRL)[1] 20-L chamber and the Fike[2] 1-m^3 chamber as measured previously by Cashdollar and Chatrathi (1992); and (iii) obtain a qualitative description of the dust dispersion process in the Siwek 20-L chamber.

2. Previous studies

The difficulty of producing a perfectly uniform dust cloud in test vessels is widely acknowledged. The high level of turbulence required at the time of ignition, rather than dust cloud uniformity, governs the selection of the ignition delay time, especially in the Siwek 20-L chamber. In test vessels, the nominal dust concentration is taken as being the representative dust concentration at the time of ignition. Therefore, the degree of error arising from this assumption can have an effect on the accuracy of the minimum explosible concentrations obtained. For this reason, it is important to have an idea of the effectiveness of dust dispersion in the test chambers at the time of ignition, so as to evaluate the assumption of dust cloud homogeneity and its effect (if any) on the accuracy of MEC data.

2.1. Optical dust probes

The effectiveness of dust dispersion in laboratory chambers and experimental mines has been investigated using optical dust probes designed at the PRL (Cashdollar, Liebman, & Conti, 1981; Liebman, Conti, & Cashdollar, 1977). These dust probes have been used to measure dust dispersion uniformity in an 8-L chamber (Hertzberg, Cashdollar, & Opferman, 1979) and in the PRL 20-L chamber and Fike 1-m^3 chamber (Cashdollar & Chatrathi, 1992). The probe operates on the principle of light attenuation. The optical dust probe used in this study measures the fraction of incident radiation that is transmitted through the dust cloud at a wavelength of ~0.95 μm. The Bouguer-law (Middleton, 1960) relates the fraction of light transmitted through the dust cloud (T) to the dust concentration (c). This law is written for dust clouds with a particle size distribution as follows:

$$T = \exp\left[-\frac{3QcL}{2\rho D_{32}}\right] \quad (1)$$

where Q = extinction coefficient or efficiency [-], c = average dust concentration [g/m^3] across the beam path, L = fixed light path length [m], ρ = density of the dust particles [g/cm^3], and D_{32} = particle surface-weighted mean diameter [μm]. The extinction coefficient/efficiency Q is a dimensionless parameter that includes the loss of light by absorption and scattering. The equation shows that the transmission is dependent on both the dust concentration and the particle size. Therefore, although it can be used to study dust dispersion uniformity, it does not measure dust concentration directly. Fig. 1 shows a cutaway view of one half of the PRL optical dust probe (Liebman et al., 1977).

2.2. Transmission data as a measure of dust cloud uniformity

If the dust cloud is perfectly uniform, the transmission measured at different points in the chamber at the time of ignition

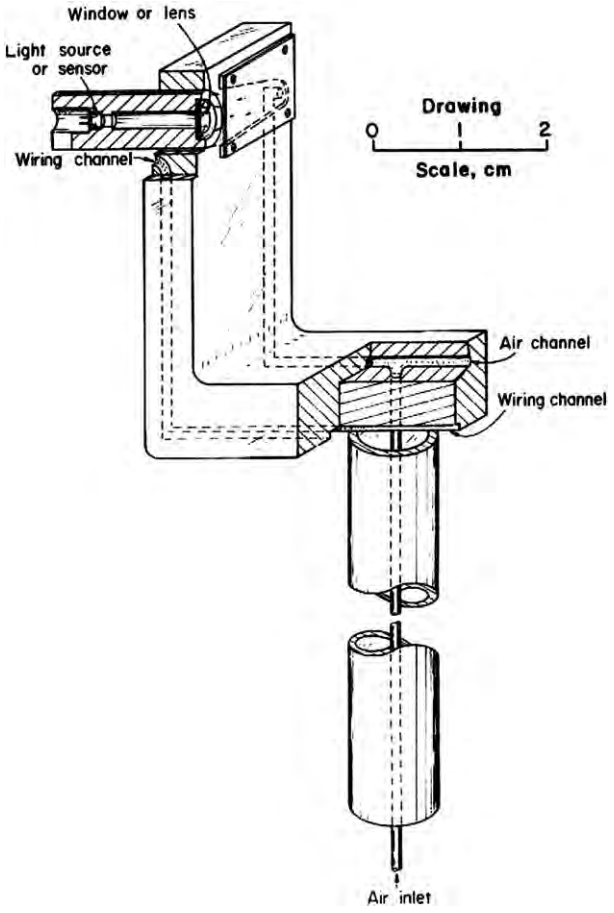

Fig. 1. Sketch of PRL optical dust probe (from Liebman et al., 1977).

[1] The Pittsburgh Research Laboratory was part of the U.S. Bureau of Mines (USBM) before transferring to the National Institute for Occupational Safety and Health (NIOSH) in October 1996.

[2] Fike Corporation, Blue Springs, Missouri, USA.

should be equal. Therefore, deviations from this ideal case can be used to quantify the degree of dust cloud homogeneity. Transmission data can also be used to make inferences about the degree of agglomeration or de-agglomeration that occurs during dispersion. Agglomeration is the tendency of the primary dust particles to stick together forming clusters of particles with larger diameters. The effective particles of a dispersed dust may exist as agglomerates of fine particles rather than as the primary particles themselves. Therefore, the degree of agglomeration is another measure of the effectiveness of dust dispersion. The degree of agglomeration or de-agglomeration can be estimated by comparing the intrinsic surface-weighted mean diameter D_{32} of the dust samples before dispersion, to that calculated from the transmission data during dispersion (Cashdollar et al., 1981).

Comparison of particle size analyses of the dust before and after dispersion can also be used to confirm the inferences made from the aforementioned procedure. In calculating D_{32} from transmission data, the dust concentration (c) in Eq. (1) is the nominal dust concentration at which the transmission data were obtained. Therefore, this method can only be used if the dispersion is fairly uniform such that the nominal dust concentration can be taken as a realistic measure of the true dust concentration. The degree of agglomeration or de-agglomeration (α) is then estimated as follows:

$$\alpha = D^{T}_{32}/D^{PSA}_{32} \quad (2)$$

in which $D^{T}{}_{32}$ is calculated from transmission data and $D^{PSA}{}_{32}$ is determined from the particle size analysis. A value of $\alpha = 1$ implies that no agglomeration has occurred during dispersion. A value of $\alpha > 1$ implies that agglomeration has occurred while $\alpha < 1$ implies that de-agglomeration and/or particle break-up has occurred during dispersion. Yet another complication is that the particle size determined by different particle size analyzers may also vary because of the different measurement techniques used.

2.3. The International Standardization Organization (ISO) and Fike 1-m^3 test chambers

Another severe limitation of the results (MEC, P_{max}, and $[dP/dt]_{max}$) obtained from the Hartmann tube (Dorsett, Jacobson, Nagy, & Williams, 1960) and other small test vessels at the time was that they could not be applied to the industrial scenario where dust handling equipment (*e.g.*, silos, mixers, pulverizers, *etc.*) with large volumes are encountered because the results do not agree with those of the large test vessels when scaled-up. The larger test vessels give more realistic estimates of the explosibility characteristics of dusts because their large volumes are more representative of the industrial situation.

In 1966, Bartknecht developed a new test procedure for the determination of the explosibility characteristics of combustible dusts in a 1-m^3 chamber (Bartknecht, 1989, p.56). Results obtained with this procedure were found to be realistic, especially in their applicability to the industrial situation. Therefore, in 1985, the International Standardization Organization (ISO) adopted the 1-m^3 test apparatus as a standard (ISO 6184/1, 1985) for the determination of the explosibility characteristics of combustible dusts. The dispersion nozzle is a 19-mm (internal diameter) tube formed into a perforated semicircular spray pipe. The holes must be 4–6 mm in diameter and the number of holes drilled in the pipe must be such that the total open area is 300 mm^2.

The spherical Fike 1-m^3 vessel varies slightly from the specifications of the ISO 1-m^3 test vessel because its dispersion pressure and ignition delay time are 32 bar (g) and 550 ms compared to 20 bar(g) and 600 ms specified in the ISO standard. However, the level of turbulence that it generates at the time of ignition (determined primarily by the initial injection pressure and ignition delay time) is comparable to that of the ISO 1-m^3 test vessel (Cashdollar & Chatrathi, 1992).

2.4. PRL 20-L chamber

The primary objective of PRL dust explosibility research is explosion prevention and protection in underground coal mines and dust-related processing facilities (Cashdollar & Hertzberg, 1985). It is therefore not surprising that the main aim of the PRL in developing a 20-L chamber was to produce accurate measurements of the MEC of combustible dusts as well as to determine inerting levels required for preventing dust explosions in coal mines. This is in contrast to the Siwek 20-L chamber, which was developed primarily for K_{St} and P_{max} tests.

The PRL explosion chamber is a near-spherical stainless steel vessel and the top of the chamber is hinged and opens fully across the chamber diameter, which facilitates ease of cleaning. Embedded in the base of the chamber is the dust reservoir in which the dust to be tested is placed and covered with a dispersion nozzle. For dispersion, the air from the 16-L reserve tank passes through a solenoid valve and then disperses the dust. The dust does not pass through the solenoid valve.

The ignition delay time, t_d, is 400 ms. The test apparatus is usually equipped with two optical dust probes located at different heights in the chamber making it the only test vessel that routinely provides some information about the uniformity of the dust cloud formed during dispersion. However, its level of turbulence, for the standard dispersion procedure, is lower than that of the Siwek 20-L chamber. For this reason, the K_{St} values obtained from this vessel cannot be used to determine venting requirements.

2.5. Effectiveness of dust dispersion in the PRL 20-L and Fike 1-m^3 chambers

Cashdollar and Chatrathi (1992) have made comparisons between the uniformity of the dust cloud formed in the PRL 20-L chamber and Fike 1-m^3 test vessel, using the PRL optical dust probes. Tests were performed over a wide range of dust concentrations. The transmission through dust clouds of Gilsonite, Pittsburgh coal and anthracite was measured at various positions in both chambers.

At the start of dispersion, the transmission is 100% until attenuation begins when the dust particles reach the probe. The most useful transmission data are those obtained at the time of ignition (*i.e.,* at the ignition delay time of the test apparatus). These were obtained by averaging (due to the rapid fluctuations with time) the transmission data over a 90-ms period prior to ignition. The Gilsonite data showed less scatter than the Pittsburgh coal data. The scatter in the data is probably due to variations in the agglomerated particle size of the air-dispersed dust.

It was also observed that the 1-m^3 transmission data were somewhat lower than the 20-L chamber at low dust concentrations. A possible explanation for this is increased agglomeration in the 20-L chamber. Furthermore, at low concentrations the dust column is short, so air may form a rat hole and have a sputtering type discharge. From the comparison between the transmission data of the Fike 1-m^3 and PRL 20-L chambers, Cashdollar and Chatrathi (1992) concluded that dispersion in the Fike 1-m^3 chamber was at least as good as that in the PRL 20-L chamber.

3. Experimental

3.1. Dusts

Gilsonite, purple K and Pittsburgh coal dusts were chosen for the dispersion tests in the Siwek 20-L chamber. Gilsonite is a natural

bitumen or asphaltite that is mined in northeastern Utah, USA. It is brittle and can be easily crushed or pulverized into a dark brown powder and is used for making paints, varnishes and linoleum. Transmission data for Gilsonite in the PRL 20-L and Fike 1-m^3 chambers are available in the literature (Cashdollar & Chatrathi, 1992).

Purple K dust is a specially coated and fluidized form of potassium bicarbonate ($KHCO_3$) used as an extinguishing agent in fire suppression. Although it is non-combustible, it has been used extensively by other researchers (Cashdollar et al., 1981) for the investigation of dispersion in test vessels using light-scattering techniques. This is primarily because it does not agglomerate readily and it tends not to adhere to the optical windows of dust probes.

Pittsburgh seam bituminous coal dust is often used as a *"standard coal"* in dust explosibility testing. In addition to the availability of extensive dust explosion data, transmission data from the PRL 20-L and Fike 1-m^3 chambers are also available. Particle size analyses of the three dusts were performed at the Minerals Engineering Centre at Dalhousie University using a Malvern Instruments 2600 Series Analyzer, which operates on the principle of laser light diffraction. The results are summarized in Table 1. The first two rows list the surface (D_{32}) and mass (D_{43}) mean diameters. The mass median diameter (D_m) is the 50% point on the mass or volume distribution curve. Note that the size data in Table 1 are somewhat different than those reported in Cashdollar and Chatrathi (1992) for the same dusts. They used a combination of sonic sieving and Coulter Counter data for their size analyses.

3.2. Dust concentrations

Five nominal dust concentrations were tested, chosen to include those for which transmission data were available for comparison, and also to include the range of dust concentrations that would be considered in a typical MEC test procedure (except for purple K since it is a non-combustible dust). The MEC of Gilsonite and Pittsburgh coal dust, as measured in the PRL 20-L chamber and Fike 1-m^3 chamber, are ~35 g/m^3 and ~80 g/m^3, respectively (Cashdollar & Chatrathi, 1992). Table 2 shows the dust concentrations used in the present work. The highest concentrations tested were limited by the necessity of having transmission values greater than 0% at the ignition time.

3.3. Apparatus

The experimental set-up is comprised of the Siwek 20-L dust explosion test apparatus, the PRL optical dust probe and a LabVIEW® – based data acquisition system. A schematic of the entire system is shown in Fig. 2.

3.3.1. Siwek 20-L chamber

The Siwek 20-L dust explosion test apparatus consists of the explosion chamber, dispersion and ignition system, pressure-measuring system and an automated control system. The explosion chamber is a spherical, stainless steel vessel with a capacity of 20 L and a pressure rating of 20 bar (g), surrounded by a water jacket for thermostatic control. At the base of the chamber is a solenoid valve (also referred to as the inlet valve) to which a 0.6-L dust storage chamber is connected. Main access into the chamber is through a 94-mm diameter opening at the top. A bayonet closure, that also holds the igniter leads, fits tightly into this opening and seals the chamber. Two 30-mm (outer diameter) flanges are fitted on the chamber; the first houses the pressure transducers, while the second is a sight glass for visual observations during tests. Other fittings attached to the explosion chamber are two valves – the exhaust valve for venting and the vacuum valve for evacuating the vessel prior to dispersion.

Table 1
Particle size analyses of the dusts used in the dispersion tests.

	Purple K	Gilsonite	Pittsburgh coal
Surface-weighted mean diameter D_{32} (μm)	18	18	43
Mass mean diameter D_{43} (μm)	44	54	76
Mass median diameter D_m (μm)	36	35	66
Weight < 75 μm (%)	83	78	59
Weight < 20 μm (%)	28	33	8
Specific surface area (m^2/m^3)	6×10^4	3×10^4	4×10^4

Table 2
Dust concentrations used in the dispersion tests.

Dust	Dust Concentration (g/m^3)
Purple K	50, 100, 150, 250, 350
Gilsonite	25, 50, 100, 150, 175
Pittsburgh coal dust	50, 100, 150, 200, 250

The Siwek 20-L chamber is supplied with two distinct dispersion nozzles, namely, the perforated annular nozzle (also known as the ring nozzle) and the rebound nozzle (ASTM, E1226, 2005a). Either of the two nozzles may be fitted into the outlet valve at the base of the chamber. However, they vary widely in their geometry and mode of operation. The perforated annular nozzle is ring-shaped with holes uniformly distributed around the surface (see Fig. 3). It has 112 holes, each 3 mm in diameter giving a total open area of approximately 792 mm^2. The dust–air mixture from the 0.6-L dust storage canister is forced through the solenoid valve and into the chamber through the holes in the annular nozzle. The rebound nozzle (see Fig. 4), also known as the deflector plate, has a total open area of 314 mm^2. Its mode of operation is dust dispersion by high impact of the dust particles on the plates of the nozzle. The dust–air mixture strikes the upper plate of the nozzle at high velocities, rebounds off the lower plate and is directed throughout the chamber. The standard dust dispersion time is 60 ms for the Siwek 20-L chamber.

The control system of the Siwek 20-L test unit is fully automated. It consists of a measurement and control unit (KSEP 332) supplied by the manufacturer (Kühner AG) and PC-based data acquisition and analysis software (KSEP 5.0d). With this system, the entire test sequence, from the pressurization of the dust storage chamber to the activation of the igniters, is controlled from a PC connected to the KSEP 332.

3.3.2. PRL optical dust probe

The version of PRL optical dust probe used in the present study was the single path length probe with air jet (Cashdollar et al., 1981; Liebman et al., 1977). The path length (distance between the optical windows of the LED and photo detector) is 38 mm. The light emitter is a gallium arsenide LED that emits near-infrared radiation with a central wavelength of 0.95 μm and a bandwidth of approximately 0.05 μm. The photo detector is a silicon photodiode, which is connected to an operational amplifier circuit to produce a voltage output linear with the input radiation of the photodiode. This probe is of the same design as that used by Cashdollar and Chatrathi (1992) in the PRL 20-L and Fike 1-m^3 chambers.

To prevent adherence of dust particles to the windows of the LED and photodiode, air exits through a 0.5-mm × 5-mm slit opening (see Fig. 1) on the windows during a test. A solenoid valve (connected to a compressed air source at 7 bar) controls this air stream. The dust probe was inserted into the Siwek 20-L chamber via a feed-through in a 30-mm diameter flange, which replaced the sight glass. The dust probe could be moved radially in the chamber, and the feed-through was sealed with O-rings. Transmission measurements were made at three positions along each of two perpendicular radial

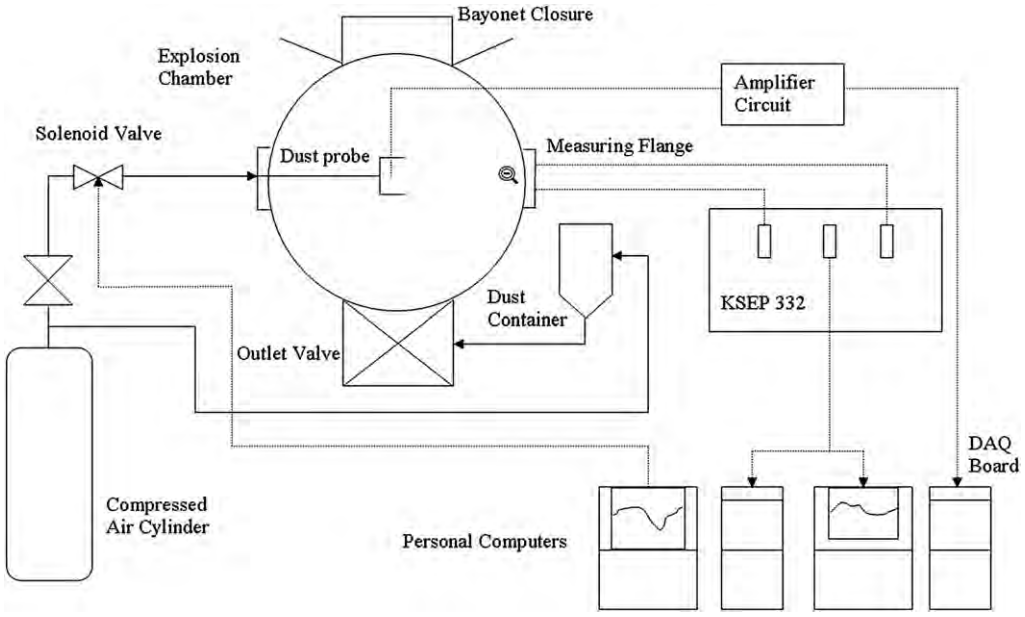

Fig. 2. Schematic of the experimental apparatus.

axes of the chamber. The first radial axis was that which extended from the sight glass to the geometric centre of the chamber while the second radial axis was that which extended from the measuring flange to the geometric centre of the chamber. For positions along the latter, the blank flange and the measuring flange were interchanged. Fig. 5 shows a horizontal cross section of the Siwek 20-L chamber indicating the dust probe locations. Positions 1, 2, and 3 were 60, 110, and 150 mm from the chamber wall. Positions 6, 5, and 4 were orthogonal to positions 1, 2, and 3 at similar distances from the chamber wall.

3.3.3. Data acquisition system

The data acquisition and control system of the entire experimental set-up consists of the automated control system of the Siwek 20-L test unit (KSEP 332) and a LabVIEW® 5.0-based computer program for optical dust probe data acquisition. LabVIEW®, which stands for Laboratory Virtual Instrument Engineering Workbench, is a programming environment in which programs are created with graphics (Wells & Travis, 1997).

The silicon photodiode is connected to an operational amplifier unit with the output voltage being in the range 0–4 V. Connection to a personal computer is through a data acquisition board. This board (National Instruments AT-MIO-16F-5) is a high performance multifunctional analog, digital and timing input/output board with a guaranteed maximum sampling rate of at least 200k samples/second (National Instruments, 1994).

The amplifier and the solenoid valve (for the dust probe) were connected to the board. The former was connected to analog channel 0, which records the voltage signal from the amplifier unit while the latter was connected to digital channel 0 to control the flow of air to the optical windows of the probe. The program could be run so as to acquire 1000 samples per second, calculate the average and display the value as "Offset/Maximum voltage". Alternatively, the program could be run to acquire data for a period specified by the operator and display the actual sample period and a graphical plot of the acquired voltage signal as a function of time. Finally, provision was made for transfer of the acquired voltage signals to a file that can be accessed through any spreadsheet application software such as Microsoft EXCEL.

3.4. Experimental procedure

A pre-weighed amount of dust was charged to the storage canister with the appropriate dispersion nozzle (rebound or perforated annular nozzle) in place. The chamber was sealed with the bayonet closure and partially evacuated to 0.4 bar (a). At this point, the LED switch of the dust probe was turned off (equivalent to 0% transmission) to record the offset voltage. The LED switch was then turned on and the maximum signal (corresponding to 100% transmission) was recorded.

The sampling rate and number of samples to be acquired were entered on the front panel of the LabVIEW® program and the toggle switch (Acquire) turned on. The control program of the Siwek test unit (KSEP 5.0d) was then initiated. The dust canister was pressurized to 20 bar (g) after which the LabVIEW® program was launched to begin data acquisition. This was done to acquire data for some time before the start of dispersion. The outlet valve then opened to allow the dust–air mixture in the dust storage canister into the explosion chamber through the dispersion nozzle, thus raising the pressure inside the chamber to 1 bar (a). The solenoid valve opened simultaneously to allow for flow of air to the optical windows of the dust probe. The sampling rate and number of samples acquired were fixed at 1000 samples/second and 3000 samples, respectively. As soon as the desired number of samples was acquired, the LabVIEW ® program displayed a dialogue box for the specification of a file name to save the data. The toggle switch was then turned off, signaling the end of data acquisition.

The file containing the acquired voltage signals was accessed *via* Microsoft EXCEL. Then the electrical offset voltage was subtracted from all the data. The acquired voltage signals were converted to % transmission out as follows:

$$T[\%] = (V_{\text{meas}}/V_{\text{max}}) \cdot 100 \tag{3}$$

where V_{meas} is the measured voltage with attenuation due to the presence of dust particles and V_{max} is the maximum voltage, corresponding to 100% transmission. The instant at which a drop in transmission (from initial 100%) was first observed was taken as point zero on the time scale. The times corresponding to the transmission data acquired prior to this point were assigned negative

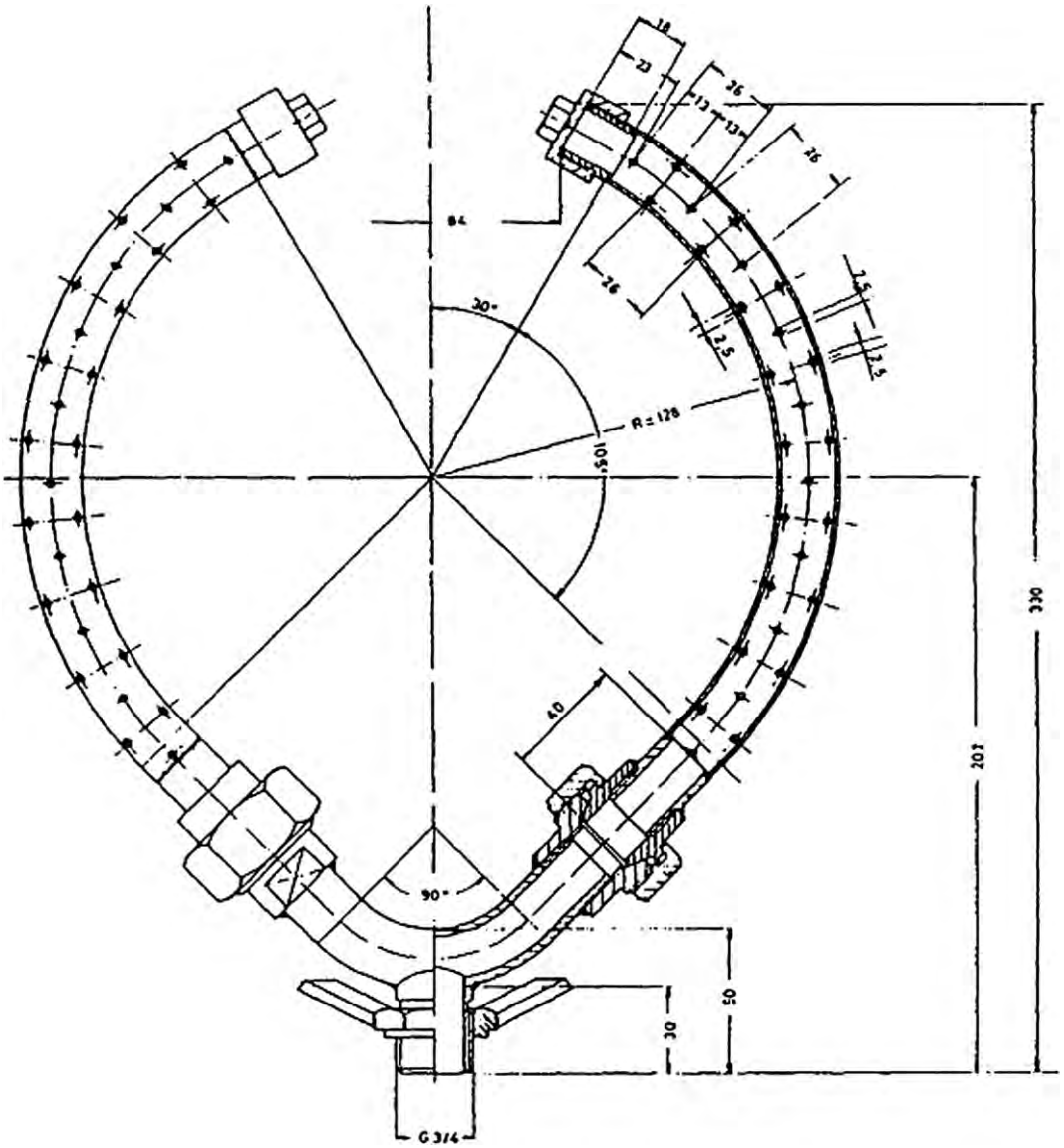

Fig. 3. The perforated annular nozzle (from ASTM standard E1226).

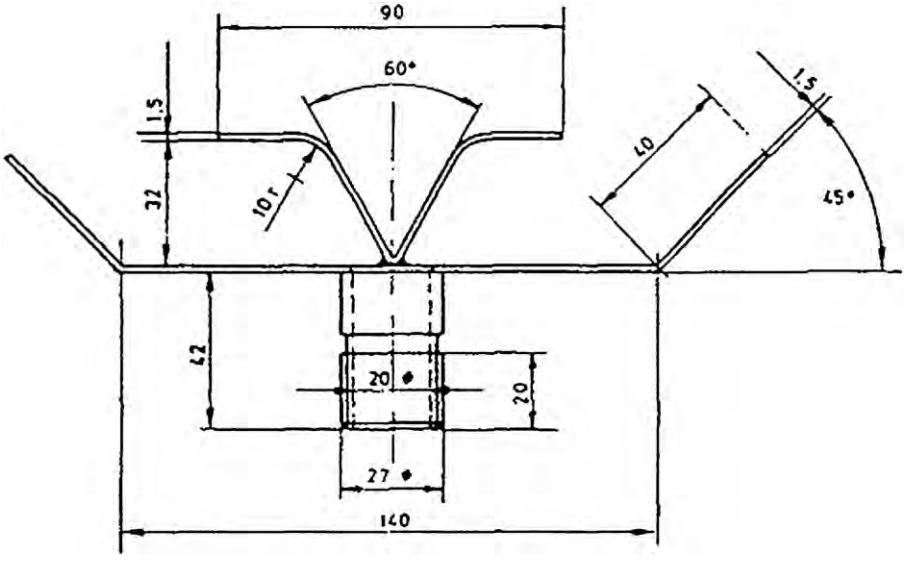

Fig. 4. The rebound nozzle (from ASTM standard E1226).

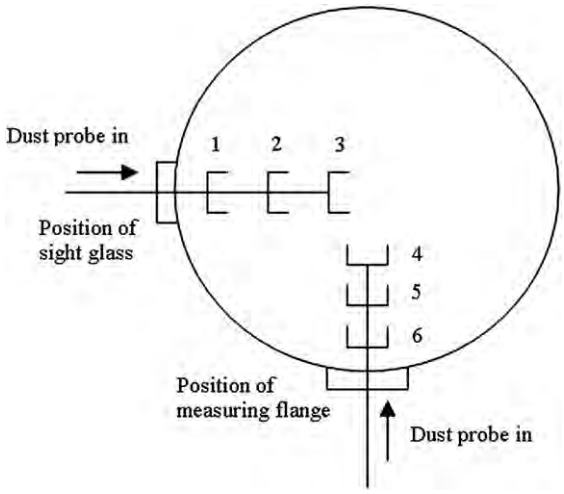

Fig. 5. Horizontal cross section of the Siwek 20-L chamber showing dust probe locations. A single probe was used in each test.

values because they represent the data acquired before the start of dispersion. Three replicate tests were performed for each of the three dusts at five dust concentrations and six dust probe locations with the two dispersion nozzles. Thus a total of 540 dispersion tests were performed.

In some cases, particle size analyses of the dust samples prior to and after dispersion were undertaken to obtain information about the effect of the dispersion process on the particle size distribution of the dusts. Therefore, for some selected dispersion tests, sufficient time was allowed for the dust particles to settle before the bayonet closure of the explosion chamber was opened after a test. The settled dust was gently scooped out of the chamber after brushing down the walls to remove any dust adhering to them. In some cases, the outlet valve was removed so that all the settled dust was easily collected from the base of the chamber.

A total of 24 post-dispersion particle size analyses were performed; 6 each for Gilsonite and purple K and 12 for Pittsburgh coal dust. The dust concentrations selected were 175 g/m^3 for Gilsonite, 250 and 350 g/m^3 for purple K and 250 and 500 g/m^3 for Pittsburgh coal. For these dispersion tests, the rebound nozzle was used.

4. Results and discussion

4.1. Transmission-time traces

Typical transmission-time traces for 25 g/m^3 Gilsonite with the rebound nozzle at probe locations 1, 2 and 3 are shown in Fig. 6. All transmission-time traces showed similar trends. At the start of data acquisition (50 ms before the start of dispersion), 100% transmission is obtained because there is no dust in the chamber and hence no attenuation of the infrared radiation from the LED. A rapid drop in transmission to some minimum value then follows as the initial "lump" or "plug" of dust is ejected from the nozzle. Transmission then increases as the dust disperses throughout the chamber, and it continues to fluctuate as the ignition delay time of 60 ms is approached.

Gilsonite is a cohesive and sticky dust that is injected into the chamber as a dense cloud and then disperses, whereas purple K is a specially coated and fluidized dust that flows easily and disperses more quickly throughout the chamber. The important point to note here is that the dusts differ in their surface properties, which can affect their patterns of flow during dispersion. This makes it difficult to generalize the description of the dust/air mixture pattern of flow in

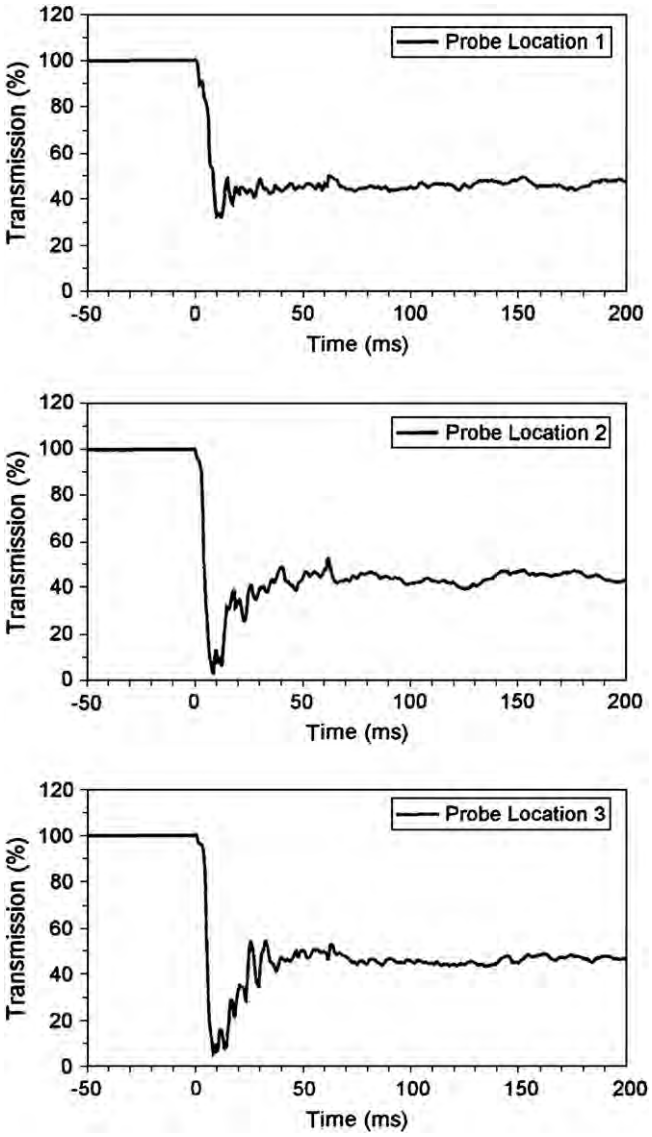

Fig. 6. Transmission-time traces for 25 g/m^3 Gilsonite with the rebound nozzle at probe locations 1, 2 and 3.

the Siwek 20-L chamber from the transmission-time traces obtained for the three dusts. Other researchers also experienced difficulties in comparing dispersions of different dusts. As reported by Eckhoff (1997), Schlapfer concluded that it was difficult to make meaningful comparisons of dispersions obtained with different dusts. He observed that dusts of different density, particle size and surface properties are dispersed in different ways if exposed to the same air blast conditions. In spite of these complications, some general conclusions regarding dust dispersion in the Siwek 20-L chamber can be deduced from the data, as described in the following sections.

4.2. Transmission at the ignition delay time

Due to rapid temporal fluctuations in the transmission data, a 20-ms time interval centred about the 60-ms ignition delay time used in the Siwek 20-L chamber (*i.e.*, 50–70 ms) was selected to determine the transmission at the time of ignition. The point zero on the time axis of the transmission-time traces does not necessarily correspond to the exact start of dispersion but rather the time that dust particles reach the probe as indicated by a sudden drop in

transmission from the initial value of 100%. Thus, point zero of the time axis shifts a little to the left. Second, in an explosion test, the igniters are activated electronically 60 ms into the dispersion process, and the igniter flame lasts about 10 ms. Several time intervals were considered (50–70, 50–80, 55–75 and 55–65 ms); however, there were no significant differences in the average transmissions (3% at the most). Hence the 50–70 ms time interval was selected. Table 3 shows the average transmissions and standard deviations in transmission, measured at all dust probe locations, at the time of ignition for Gilsonite, purple K, and Pittsburgh coal, for all dust concentrations and the two dispersion nozzles. In the table, each of the data values listed for a particular probe position and dust concentration is the average of three replicate tests.

Repeatability refers to the run-to-run variations among replicate tests under the same experimental conditions. The % deviations of the transmission at the time of ignition obtained from each experimental run from the average value over three replicate tests were calculated. The transmission at the time of ignition for 98 of the 540 experimental runs exceeded 20% deviation. However, the majority of the deviations outside this range were obtained for high dust concentrations of Gilsonite and purple K, where the transmission was very low. These low transmissions account for deviations as large as 50% or 100%. For example, a 1% transmission at the ignition delay time obtained from one run gives a deviation of −50% if the average transmission at ignition obtained over three replicate tests was 2%. Nevertheless, 82% of the 540 experimental runs were within a 20% deviation and it is concluded that the repeatability of the transmission measurements was reasonable. If only the transmission data greater than 10% are considered, 90% of 414 runs were within 20% deviation.

Table 3
Average transmissions and standard deviations in transmission at the time of ignition for Gilsonite, purple K and Pittsburgh coal dust with the rebound (R) and perforated annular (A) nozzles.

Gilsonite	Transmission [%]									
Dust Concentration [g/m^3]	25		50		100		150		175	
Dust probe location	R	A	R	A	R	A	R	A	R	A
1	46	48	31	35	11	19	5	8	3	4
2	46	35	32	34	20	18	9	11	4	6
3	49	32	32	34	15	19	9	9	7	6
4	32	49	29	39	15	20	6	15	5	10
5	41	47	32	35	17	18	8	9	5	10
6	54	40	32	32	12	21	4	12	2	12
Mean transmission	45	42	31	35	15	19	7	11	4	8
Standard deviation	8	7	1	2	3	1	2	3	2	3
Purple K										
Dust Concentration [g/m^3]	50		100		150		250		350	
Dust probe location	R	A	R	A	R	A	R	A	R	A
1	61	64	40	46	27	27	8	10	2	0
2	60	61	39	44	29	30	5	8	0	1
3	57	63	41	38	25	29	7	7	0	0
4	58	57	42	48	30	22	9	7	3	1
5	60	66	42	37	25	22	9	7	0	0
6	62	65	42	47	28	33	13	13	1	4
Mean transmission	60	63	43	43	27	27	9	9	1	1
Standard deviation	2	3	1	5	2	4	3	2	1	2
Pittsburgh coal										
Dust Concentration [g/m^3]	50		100		150		200		250	
Dust probe location	R	A	R	A	R	A	R	A	R	A
1	56	65	41	51	33	39	25	30	21	27
2	56	63	43	44	28	39	27	27	25	23
3	51	61	41	46	28	31	23	27	30	21
4	55	66	48	54	37	37	29	30	28	25
5	60	69	46	50	39	39	33	25	26	24
6	60	57	45	44	38	35	34	39	26	29
Mean transmission	56	64	48	48	34	37	29	30	26	25
Standard deviation	3	4	3	4	5	3	4	5	3	3

4.3. Variations in spatial uniformity of dispersion for rebound and perforated annular nozzles

For a perfectly uniform dust cloud, there should be no variation in local dust concentration throughout the chamber volume at the time of ignition. From Bouguer's law, Eq. (1), we know that transmission is a measure of dust concentration; hence for a perfectly uniform dust cloud there should be no variation in the transmission at the time of ignition obtained at different locations throughout the chamber volume. However, the transmission is also a function of the particle size and, therefore, the agglomeration of the dust at different locations.

Fig. 7 shows a semi-logarithmic plot of transmission at the time of ignition as a function of the nominal dust concentration for Gilsonite at all six dust probe locations with the rebound and perforated annular nozzles. Each of the plotted data points is the average of the three runs at one position and concentration (from Table 3). Not all of the data points at the six locations can be seen on the graph at each concentration, due to overlap of the data. Transmission generally decreases with increasing dust concentration in accordance with Bouguer's law. For both nozzles, the transmission approached zero as the dust concentration increased to 175 g/m^3. Further increases in dust concentration would give zero transmission at the time of ignition and it is for this reason that higher dust concentrations were not tested.

On the semi-logarithmic plot of Fig. 7, it appears that the greatest variation is at the highest concentration. However, on an absolute basis (see Table 3), the widest variation in transmission for both nozzles was obtained at the lowest dust concentration tested (*i.e.* 25 g/m^3), which is not surprising because as the quantity of dust in the chamber decreases so the probability of obtaining equal portions of dust at different locations also decreases. There do not appear to be any significant differences between the results obtained from the two nozzles. Variations in spatial uniformity from both nozzles are similar as indicated by the standard deviations in transmissions obtained at the time of ignition at the different dust probe locations for each dust concentration (see Table 3). The low standard deviations also indicate good uniformity of dispersion with both nozzles.

However, the rebound nozzle gave somewhat lower transmission values than those of the perforated annular nozzle at the highest Gilsonite concentrations tested. A possible explanation for this is that the rebound nozzle is more efficient in breaking up agglomerates of this dust. With purple K dust (Fig. 8), transmission at the time of ignition decreased with increasing nominal dust concentration at all six probe locations until near-zero transmissions were obtained at a dust concentration of 350 g/m^3 for both nozzles. As in Fig. 7, each of the plotted data points is the average of the three runs at one position and concentration. Again, there were no significant differences in the transmission data at the various locations for the two nozzles. Furthermore, low standard deviations in transmission (Table 3) indicated that both nozzles gave good uniformity of dispersion. Similar results were found for Pittsburgh coal dust (Fig. 9 and Table 3). For both the purple K and Pittsburgh coal, the transmission data for the two nozzles were essentially the same.

From the results obtained for the three dusts, it can be concluded that good uniformity of dispersion was achieved using either the perforated annular nozzle or the rebound nozzle for dispersion. Also, there was no significant difference in the variation in spatial uniformity from dispersion with either nozzle, despite their differences in geometry and mode of operation. This is consistent with the conclusions of Siwek (1988) and Eckhoff (1977) that both nozzles produce approximately the same degrees of dust dispersion. Siwek's conclusion was based on high-speed motion pictures of dust dispersion with the two nozzles in a Plexiglas model of the chamber that allowed for visualization of the

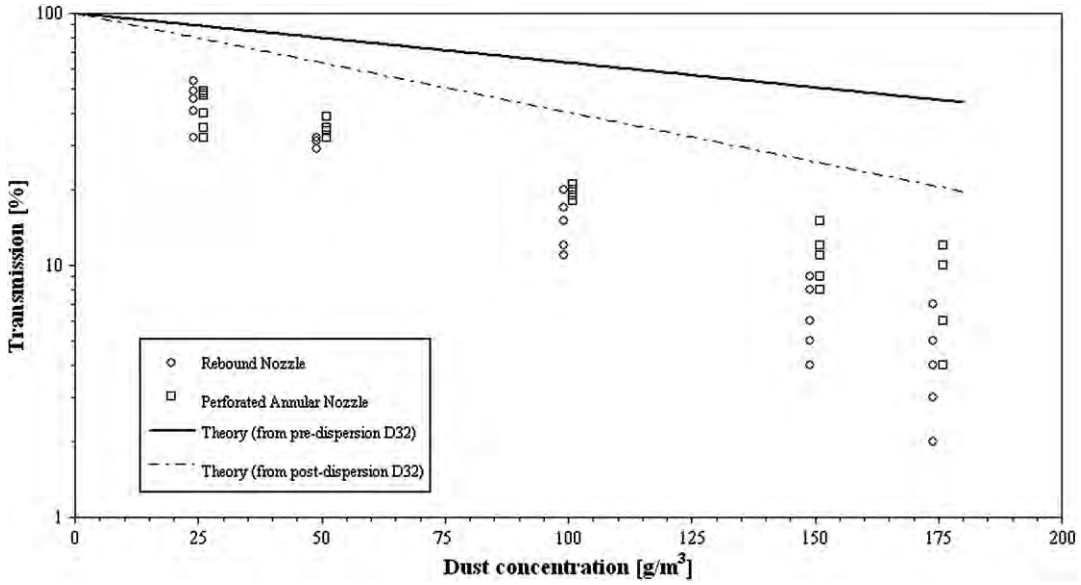

Fig. 7. Semi-logarithmic plot of Bouguer's law (calculated using pre- and post-dispersion D_{32}) and experimental transmission data as a function of dust concentration for Gilsonite.

dispersion process, similar to the method used by Eggleston and Pryor (1967) for the 1.2-L Hartmann tube.

Figs. 7–9 and Table 3 also show that for each set of experiments with the three dusts there is no specific pattern in the distribution of the transmission data across the six dust probe locations. The inference that can be made from this is that the dispersion obtained with the two nozzles should not affect the rate of flame propagation in the Siwek 20-L chamber.

The conclusion that there are no differences in the variations in spatial uniformity obtained with the rebound and the perforated annular nozzle was not simply based on visual inspection of the results shown in Table 3. It was shown statistically through an analysis of variance (ANOVA). ANOVA is a standard procedure for making statistical inferences about the equality of two or more population means. In this case, the two populations are the variations in spatial uniformity obtained with the rebound and the perforated annular nozzles (Table 3). Details of the test procedure can be found in, for example, Montgomery and Runger (1999). The results showed that the computed value of the test statistic (F) was smaller than the critical value for the rejection region (F_{critical}). Therefore the null hypotheses of equality of the rebound and perforated annular nozzle population means for the three dusts were accepted.

4.4. Predictions from Bouguer's law

Figs. 7–9 show semi-logarithmic plots of the theoretical and experimental transmission data as a function of dust concentration for Gilsonite, purple K, and Pittsburgh coal dust. Two theoretical transmissions were calculated from Eq. (2) using an extinction efficiency $Q = 1.5$ and path length $L = 0.038$ m (distance measured

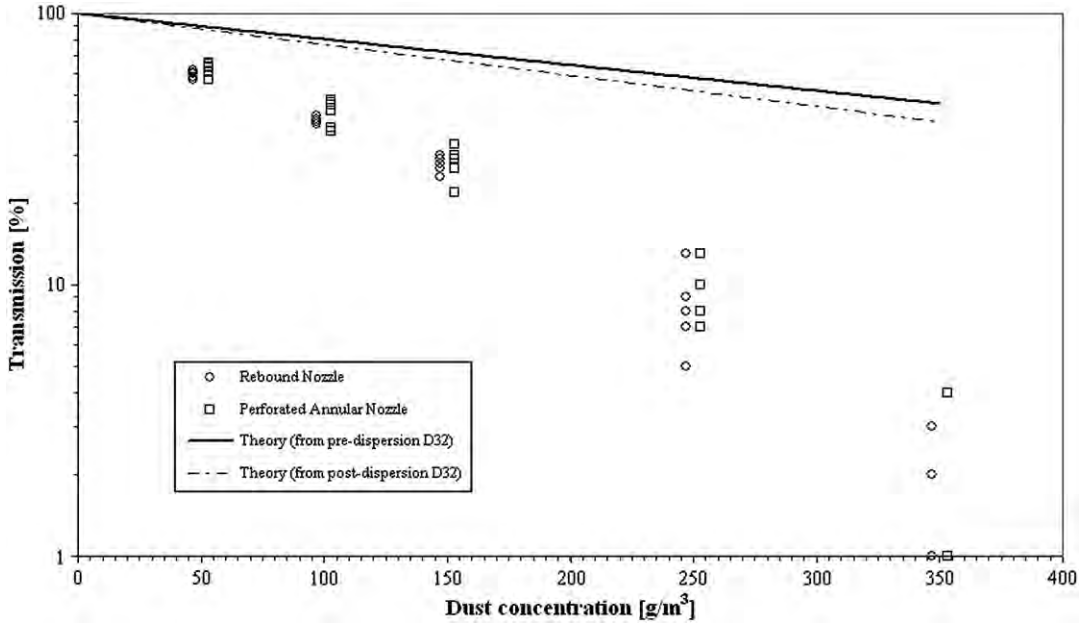

Fig. 8. Semi-logarithmic plot of Bouguer's law (calculated using pre- and post-dispersion D_{32}) and experimental transmission data as a function of dust concentration for purple K.

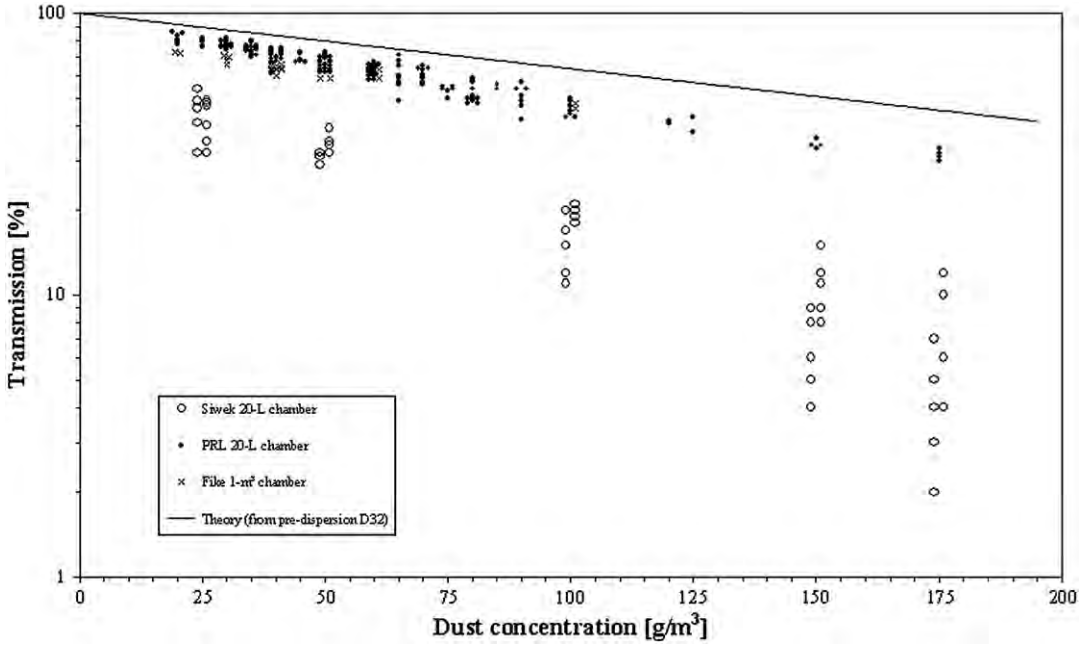

Fig. 9. Semi-logarithmic plot of Bouguer's law (calculated using pre- and post-dispersion D_{32}) and experimental transmission data as a function of dust concentration for Pittsburgh coal.

between the dust probe windows), from Cashdollar et al. (1981). The particle densities used were ρ = 1.05, 2.17, and 1.34 g/cm^3 for Gilsonite, purple K and Pittsburgh coal dust, respectively. The first prediction (shown as the solid lines in Figs. 7–9) was calculated using particle diameters of D_{32} = 18, 18, and 43 μm for Gilsonite, purple K and Pittsburgh coal dust, respectively, obtained from the pre-dispersion particle size analyses shown in Table 1. It can be seen from Figs. 7–9 that the experimental transmission data of the three dusts generally follow a linear relationship as expected from Bouguer's law. However, the experimental transmission data for the three dusts were significantly lower than their respective theoretical relationships (shown as solid lines in Figs. 7–9).

There are several possible explanations for the significant deviations of the experimental data from the theoretical lines. First, the theoretical lines as determined from Bouguer's law are based on a homogeneously dispersed dust cloud scenario, in which case the nominal dust concentration is the true or actual dust concentration. The transmission measurements at the various locations in the chamber showed good uniformity (Table 3), and it is difficult to see how the concentrations at these locations could all be greater than the nominal value. Second, the extinction efficiency (Q) is a function of particle size, wavelength of incident radiation and the complex refractive index of the particles. For particles larger than the wavelength of incident radiation, it varies between 1 and 2 depending on the type of light source and detector used. Based on experimental measurements, the extinction efficiency for the dust probes is 1.5 with an uncertainty of ±0.2 (Cashdollar et al., 1981), which is a relatively small uncertainty. An even larger uncertainty exists with the surface-weighted mean diameter (D_{32}), which may vary widely for the same dusts as a result of differences in particle size measuring techniques. Third, the air jet that sweeps across the optical windows of the dust probe does not keep the windows totally dust free during dispersion. Dust coatings on the optical windows of the probe absorb light, which will lead to a decrease in transmission.

Finally, there is the possibility of the dust particle size distribution changing during the dispersion process. The D_{32} values used in computing the theoretical transmission data (solid lines in Figs. 7–9) were determined from particle size analyses of the dust samples prior to dispersion (Table 1). As discussed in section 2.2, it is possible to make inferences about the degree of agglomeration during the dispersion process by comparing D_{32} before dispersion, and D_{32} calculated from the transmission data during dispersion. However, agglomeration can only increase the particle size, not decrease it. Table 4 shows that the particle sizes for all three dusts calculated from the transmission data are much smaller than their original sizes before dispersion. The values of α (*i.e.* the degree of agglomeration/de-agglomeration or break-up) calculated from Eq. (3) were about 0.2 for all three dusts. These values of α are significantly less than 1, which implies that particles break-up during dispersion. It is unlikely that the uncertainties in comparing the theoretical and experimental transmission data discussed earlier in this section could account for the very low values of α obtained. Further, the manufacturer of the Siwek 20-L test apparatus warns that the combination of the outlet valve and the dispersion nozzle might have a grinding effect on the dust particles leading to particle size reduction in the course of dispersion (Adolf Kühner, 1994).Therefore, the next logical step was to measure the particle size of the dust collected after dispersion.

4.5. Comparisons of particle size analyses before and after dispersion

The discussion presented here is based on results obtained using the rebound nozzle. Since transmission data for the rebound and

Table 4
Comparison of pre-dispersion dust size measured by particle size analyzer and size calculated from experimental transmission data.

Dust	Dust Concentration (g/m^3)	D_{32} from particle size analyses (μm)	D_{32} calculated from transmission data (μm)
Gilsonite	25–175	18	3–5
Purple K	50–350	18	3–5
Pittsburgh coal dust	50–250	43	6–12

perforated annular nozzles are similar with both being significantly lower than the theoretical predictions (solid lines in Figs. 7–9), the effect of particle size reduction with both nozzles is expected to be comparable. From particle size analyses before and after dispersion for the three dusts there was clear evidence of particle size reduction resulting from the process of dispersion. Several parameters can be used to characterize the particle size of a dust. The surface-weighted mean diameter D_{32}, is the most appropriate for incorporation into Bouguer's law because light scattering is a surface phenomenon. Therefore, estimations of the degree of particle size reduction were based primarily on comparisons between D_{32} obtained before and after dispersion. However, estimations based on D_m, the mass median diameter, and D_{43}, the mass mean diameter, also give comparable results.

From particle size analyses performed on four different portions of the Gilsonite sample prior to dispersion, it was clear that intra-sample variation in particle size was small. The post-dispersion particle size analyses for six experimental runs at a concentration of 175 g/m^3 also showed consistency from run-to-run. Using D_{32} values for comparison, the post-dispersion size was about 50% of the original size for the Gilsonite, as listed in Table 5. Similarly, the results of the particle size analyses for Pittsburgh coal dust before and after dispersion showed consistency from run-to-run. For the coal, there were six dispersions at 250 g/m^3 and six dispersions at 500 g/m^3. Using D_{32} values for comparison, the post-dispersion size was about 40% of the original size for the Pittsburgh coal, as listed in Table 5. There was also no significant difference in the size analyses after dispersions at the two dust concentrations.

However, in the case of purple K, there was evidence of particle size reduction but not as significant as that obtained with Gilsonite and Pittsburgh coal dust. The particle size analyses before dispersion showed small intra-sample variation in particle size and again consistency was obtained in the post-dispersion particle size analyses from run-to-run. Using D_{32} values for comparison, the post-dispersion size was about 80% of the original size, or alternatively, the reduction in particle size was about 20%. Since Gilsonite and purple K particle sizes are comparable in terms of fineness (Tables 1 and 5), and significant particle break-up was obtained with the former but not the latter, it is suggested that purple K might be more difficult to break or fragment than Gilsonite. Particle size analyses for purple K before and after dispersion also indicated that the post-dispersion values of D_{32} are essentially the same at the two different dust concentrations (250 and 350 g/m^3) tested. This, along with the coal data, suggests that the effect of dust concentration on the extent of particle size reduction was negligible.

The next question was: what was causing the particle size reduction – the dispersion nozzle or the outlet valve of the dispersion reservoir? To evaluate this, a dispersion test with Pittsburgh coal was performed with the rebound dispersion nozzle removed. The results were somewhat surprising because they showed that as much particle size reduction occurred without the dispersion nozzle as with the nozzle. This suggests that high velocity flow of the dust/air mixture through the outlet valve, not the action of the dispersion nozzle, is largely responsible for the reduction in particle size.

Table 5
Comparison of particle size analyses before and after dispersion for the three dusts.

	Before dispersion	After dispersion
Gilsonite		
D_{32} (μm)	18	9
D_{43} (μm)	54	22
Purple K		
D_{32} (μm)	18	15
D_{43} (μm)	44	35
Pittsburgh coal		
D_{32} (μm)	43	17
D_{43} (μm)	76	40

The outlet valve of the Siwek 20-L chamber is unique in its design and differs from conventional ball or solenoid valves. It is opened and closed pneumatically by means of an auxiliary piston, which is enclosed in a valve casing attached to the opening at the base of the chamber such that the piston of the outlet valve covers the opening when the valve is in the closed position. When the valve opens, the piston plunges downward to create an annular space for the dust to flow into the chamber and returns to its original position when the valve closes. It is the forced flow of the dust/air mixture through the annular space existing between these two concentric circles that leads to compaction or squashing and grinding of the dust particles as they rub against the edges of the piston. As a result, particle break-up occurs before the dust enters the chamber through the dispersion nozzle. This may explain why the extent of particle size reduction obtained with purple K was much lower than that obtained with Gilsonite and Pittsburgh coal dust. Purple K is a specially coated and fluidized dust that flows easily. Therefore, friction between the dust particles and the edges of the piston during flow is reduced and this leads to a corresponding decrease in the extent of particle break-up. Specific details of the outlet valve are given elsewhere (Kalejaiye, 2001). Therefore, to thoroughly evaluate the effect of particle size reduction in the Siwek 20-L chamber, pre- and post-dispersion analyses should be made for tests with additional sizes and types of dusts and correlated to a material frangibility parameter.

Using the post-dispersion surface-weighted mean diameters (from Table 5) of 9, 15, and 17 μm obtained for Gilsonite, purple K and Pittsburgh coal dust, respectively, new theoretical transmissions were calculated from Bouguer's law. These are shown as the dotted lines in Figs. 7–9. It can be seen that better agreement exists between the experimental data and the post-dispersion theoretical lines, especially for Gilsonite and Pittsburgh coal dust. However, the experimental data are still lower than even the post-dispersion theory lines.

4.6. Comparisons with transmission data from the PRL 20-L and Fike 1-m^3 chambers

Figs. 10–12 are semi-logarithmic plots of experimental transmission data as a function of dust concentration for Gilsonite, purple K, and Pittsburgh coal dust from the Siwek 20-L chamber together with data previously reported from the PRL 20-L and Fike 1-m^3 chambers (Cashdollar & Chatrathi, 1992) for the Gilsonite and coal. The purple K data from the PRL 20-L chamber in Fig. 11 were not previously published.

The theoretical lines displayed are those calculated for the current work based on pre-dispersion values of D_{32} (*i.e.* the solid lines shown in Figs. 7–9), since the particle size distributions of the Gilsonite and Pittsburgh coal dust samples used in previous work (Cashdollar & Chatrathi, 1992) are comparable to those used in the current work. The PRL 20-L data for purple K in Fig. 11 were measured recently using a sample from the same purple K that had been used for the Siwek 20-L data. For Gilsonite (Fig. 10), the transmission data in the PRL and Fike chambers generally followed a linear relationship as expected from Bouguer's law. Both showed good uniformity of dispersion (*i.e.* small variations in spatial uniformity) comparable to that obtained in the Siwek 20-L chamber. Note that the scatter in the Siwek 20-L data is exaggerated by the semi-logarithmic plots. Similarly for purple K (Fig. 11) and Pittsburgh coal dust (Fig. 12), the transmission data in the PRL and Fike chambers generally followed a linear relationship. The PRL 20-L chamber data indicated good uniformity of dispersion comparable to that of the Siwek 20-L

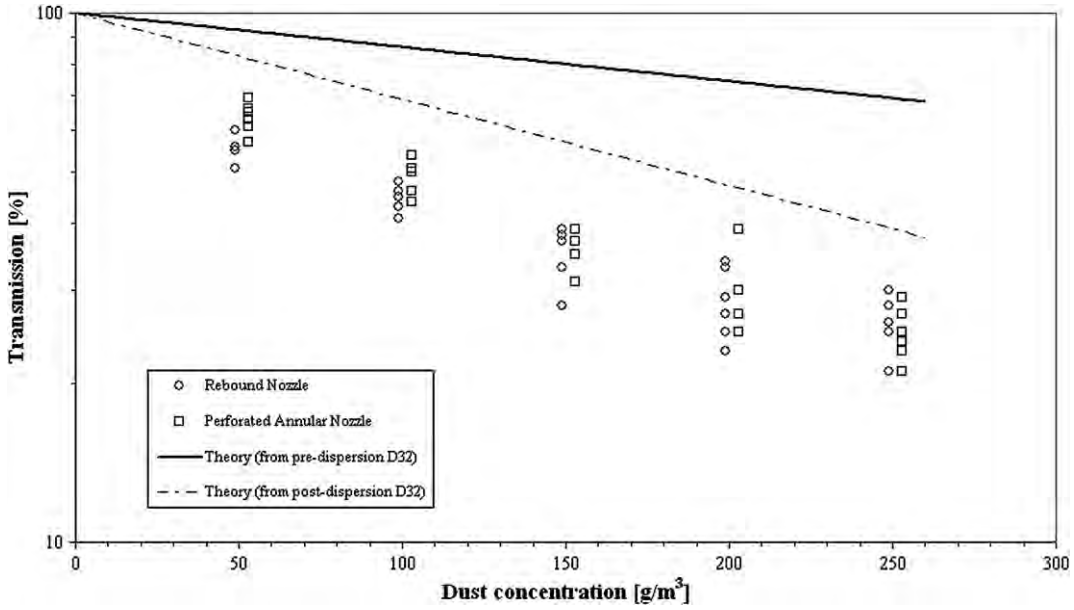

Fig. 10. Semi-logarithmic plot of transmission (%) versus dust concentration (g/m^3) data for Gilsonite from the Siwek 20-L and PRL 20-L chambers.

chamber at low dust concentrations. At the higher dust concentrations for the Pittsburgh coal, larger variations in dust probe transmission data were observed with the PRL 20-L chamber data. These wide variations (or scatter of the data) are attributed to variations in the agglomerated particle size of the air-dispersed dust. In particular, PRL 20-L data shown in Fig. 11 were acquired over a period of many years in which case there might have been variations in the actual particle size distribution of the dusts, which could lead to variations in the agglomerated particle sizes of the air-dispersed dust and hence scatter in the transmission data. It should also be noted that the PRL 20-L and Fike 1-m^3 data points were for individual dispersion tests while the Siwek 20-L data points (Table 3 and Fig. 12) were an average of three tests at each concentration and location.

The Fike 1-m^3 chamber transmission data (Figs. 10 and 12) showed good uniformity of dispersion comparable to that of the Siwek 20-L chamber. However, transmission data were obtained using two PRL optical dust probes at fixed locations both in the same hemisphere of the chamber and limited data points, relative to the number of data points available from the PRL 20-L chamber.

From Figs. 10–12 it is obvious that the Siwek 20-L transmission data are significantly lower than the PRL and Fike transmission data at all the dust concentrations tested. For Gilsonite (Fig. 10), the PRL

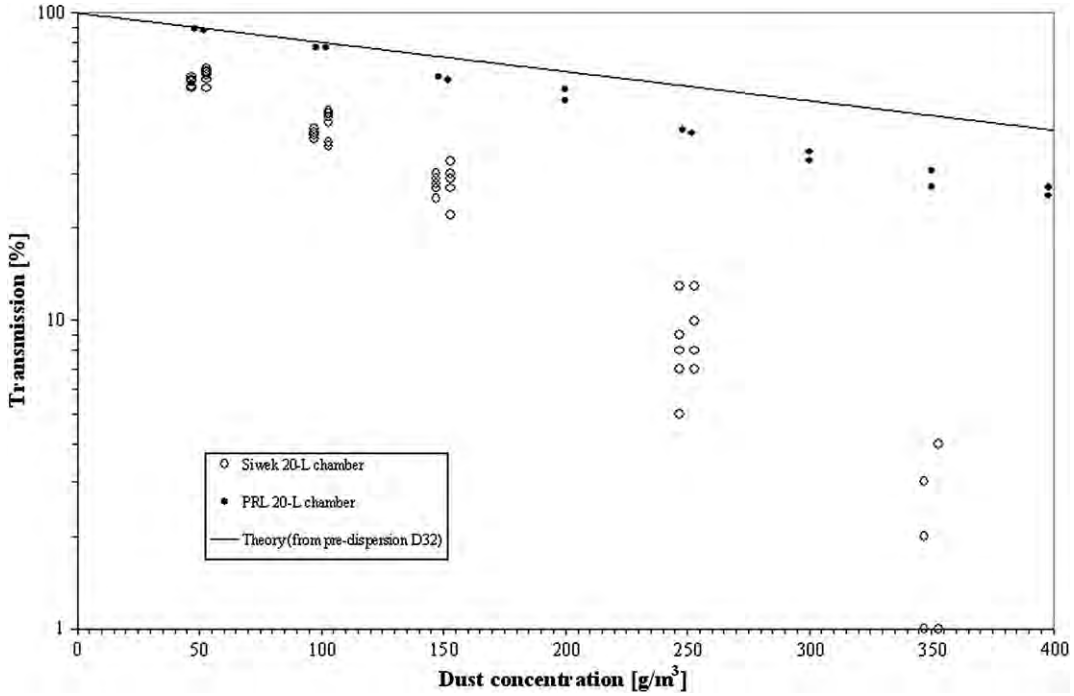

Fig. 11. Semi-logarithmic plot of transmission (%) versus dust concentration (g/m^3) data for Pittsburgh coal dust from the Siwek 20-L, PRL 20-L and Fike 1-m^3 chambers.

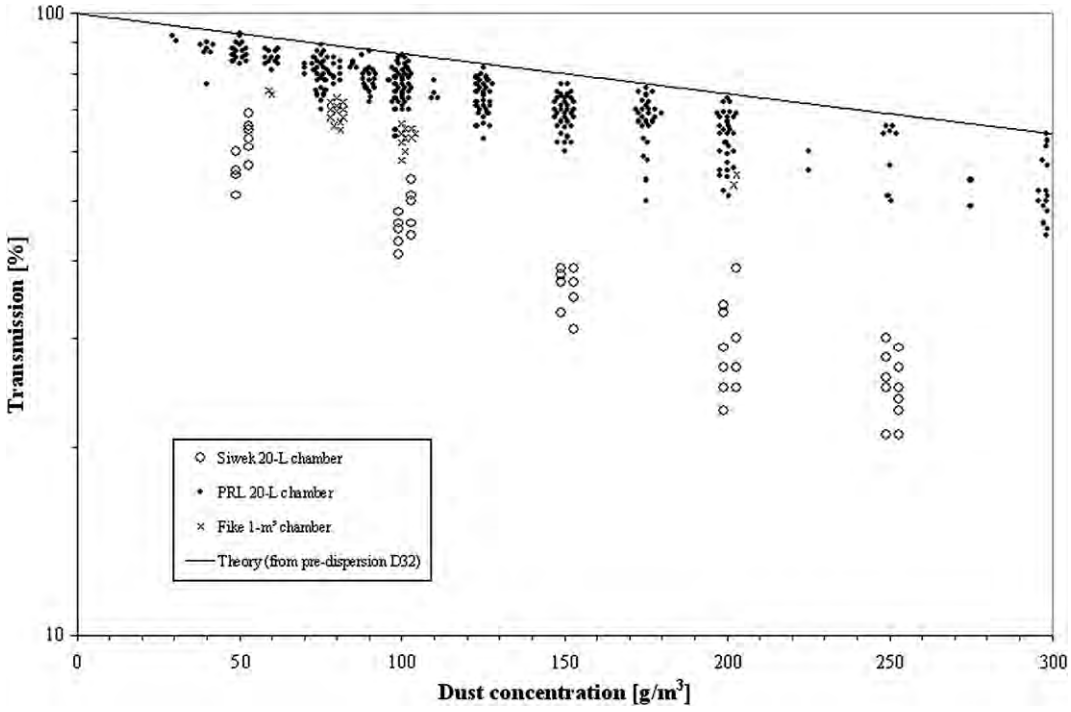

Fig. 12. Semi-logarithmic plot of transmission (%) versus dust concentration (g/m^3) data for Pittsburgh coal dust from the Siwek 20-L, PRL 20-L and Fike 1-m^3 chambers.

and Fike transmission data are slightly below the theoretical line, unlike the Siwek 20-L data, where the deviations from the theoretical relationship are significant. It has been confirmed in the preceding section of the current work that the significant reduction in particle size obtained during dispersion in the Siwek 20-L chamber was largely responsible for the wide deviations from the theoretical relationship.

However, there is no clear evidence of particle size reduction in the PRL and Fike chambers based on the transmission data. In a previous investigation with the PRL 20-L chamber, Pittsburgh bituminous coal was dispersed at concentrations of 400 and 600 g/m^3, and multiple size analyses were performed for the dust before and after dispersion (Cashdollar, 1996). The mean diameters D_{32} and D_{43} after dispersion were 93% and 95% of their original values, respectively. This shows that there was almost no particle size reduction for the Pittsburgh coal in the PRL 20-L chamber. There was evidence of particle break-up during dispersion of TNT explosives dusts in the PRL 20-L chamber (Cashdollar, Hertzberg, and Green, 1992; Hertzberg, Cashdollar, Zlochower, & Green, 1992), but this was for coarser sizes.

Figs. 10 and 12 show no significant differences between the PRL 20-L and Fike 1-m^3 data implying that little or no particle size reduction occurs in the Fike 1-m^3 chamber during dispersion. The level of turbulence generated in the Fike 1-m^3 chamber is assumed to be comparable to that of the ISO 1-m^3 test vessel which, until recently, was assumed to be comparable to that obtained in the Siwek 20-L chamber. However, a recent study by Dahoe, Cant, Pegg, and Scarlett (2001) has shown that significantly different turbulence levels occur in the two vessels at their respective ignition delay times. The turbulence level in the Siwek chamber at 60 ms is higher than the turbulence level in the ISO 1-m^3 chamber at its standard ignition delay of 600 ms. It is only at a later time of 200 ms that the turbulence level in the Siwek chamber is comparable to that in the ISO 1-m^3 chamber. In addition, the dust was subjected to a pressure of 32 bar (g) prior to dispersion in the Fike 1-m^3 test apparatus and 20 bar(g) in the Siwek 20-L chamber. The dispersion nozzle of the Fike 1-m^3 chamber is similar in design to the perforated annular nozzle of the Siwek 20-L chamber. Surprisingly, significant particle size reduction was obtained for Gilsonite and Pittsburgh coal dust in the latter but not in the former. However, the dispersion valve of the Fike 1-m^3 chamber is a 19-mm pneumatically operated ball valve (Cashdollar & Chatrathi, 1992) that is not expected to have any significant effect on the dust as it flows through it. This strengthens the argument put forward in section 4.5 that the action of the outlet valve contributes the most to the reduction in particle size obtained in the Siwek 20-L chamber. Nevertheless, the effect of flow through the dispersion nozzle and the high levels of turbulence generated are relatively minimal in terms of particle size reduction.

5. Conclusions

This research evaluated the dust dispersion effectiveness in the Siwek 20-L chamber, which is widely used for dust explosibility studies. Dispersion tests were performed in the chamber with three dusts, namely, Gilsonite, purple K and Pittsburgh coal using the rebound and perforated annular dispersion nozzles. Transmission data were obtained from six different locations in the chamber using a PRL optical dust probe. Transmissions at the time of ignition were obtained by averaging the transmission-time data over a 20-ms interval centred about the standard ignition delay time of the chamber (60 ms). Variations in spatial uniformity of dispersion were determined by calculating the mean standard deviations of the transmissions obtained at the time of ignition from the six dust probe locations with both the rebound and perforated annular nozzles. From these results, the following conclusions are drawn.

- Transmission generally decreased with increasing dust concentration for the three dusts, as predicted from Bouguer's transmission law.
- Variations in spatial uniformity obtained with both nozzles were found to be essentially the same for the three dusts. This statement is consistent with the conclusions of Eckhoff (1997) and Siwek

(1988) that the rebound nozzle produces degrees of dust dispersion similar to those of the perforated annular nozzle. The low standard deviations obtained showed that good uniformity of dispersion was achieved for the three dusts with both nozzles.

- Comparisons were made between experimental transmission data obtained for the three dusts in the current work and the theoretical values calculated from Bouguer's law, Eq. (1). The experimental transmissions were significantly lower than the theory for all three dusts at all the dust concentrations tested. The surface-weighted mean particle diameters for the dispersed dusts were calculated from the transmission data and compared to the values obtained from the Malvern particle size analyzer prior to dispersion. The results indicated that significant reduction in particle size had occurred during the course of dispersion.
- Particle size analyses were performed for the dusts before and after dispersion to confirm this apparent size reduction. The comparisons showed that the size after dispersion was about 50%, 80%, and 40% of the original size for Gilsonite, purple, and Pittsburgh coal dust, respectively. The effect of dust concentration on the extent of particle size reduction was found to be negligible. The surface-weighted mean diameters of the post-dispersion dusts were then used to compute new theoretical lines from Bouguer's law. Better agreement was obtained between these post-dispersion size values and the experimental transmission data, especially for Gilsonite and Pittsburgh coal dust.
- Comparisons were made between the Siwek 20-L transmission data of the current work and those obtained in the PRL 20-L and Fike 1-m^3 chambers for Gilsonite and Pittsburgh coal dust. The variations in spatial uniformity observed from the transmission data of the Siwek, PRL and Fike chambers showed that, in general, good and comparable uniformity of dispersion was obtained in the three vessels. However, there was no evidence of particle size reduction in the Fike and PRL chambers in contrast with the Siwek chamber where significant reductions in particle size occurred during dispersion.
- Particle size reduction in the Siwek 20-L chamber was attributed to the unique design of its outlet (dispersion) valve and its shearing action on the dust particles as they flow through. This contention is strengthened by warnings from the manufacturers of the Siwek 20-L test apparatus that the combination of the outlet valve and the dispersion nozzle might have a grinding effect on the dust particles, leading to a reduction in particle size. However, the current work has shown that reduction in particle size is largely due to the action of the outlet valve with the contribution from the dispersion nozzle being minimal.

References

Adolf Kühner, A. G. (1994). *Operating instructions for the 20 litre apparatus 5.0*. Basel, Switzerland: Ciba-Geigy AG.

ASTM. (2005a). *E1226–00, Standard Test Method for Pressure and Rate of Pressure Rise for Combustible Dusts*. Annual Book of ASTM Standards, 14.02, 334–345.

ASTM. (2005b). *E1515–03a, Standard Test Method for Minimum Explosible Concentration of Combustible Dusts*. Annual Book of ASTM Standards, 14.02, 487–495.

Bartknecht, W. (1989). *Dust explosions: Course, prevention, protection*. Berlin: Springer–Verlag.

Cashdollar, K. L. (1996). Coal dust explosibility. *Journal of Loss Prevention in the Process Industries, 9*, 65–76.

Cashdollar, K. L., & Chatrathi, K. (1992). Minimum explosible dust concentrations measured in 20-L and 1-m^3 chambers. *Combustion Science and Technology, 87*, 157–171.

Cashdollar, K. L., & Hertzberg, M. (1985). 20-L explosibility test chamber for dusts and gases. *Review of Scientific Instruments, 56*, 596–602.

Cashdollar, K. L., Hertzberg, M., & Green, G. M. (1992). *Hazards of explosives dusts: Particle size effects*, Pittsburgh Research Center Internal Report No. 4901.

Cashdollar, K. L., Liebman, I., & Conti, R. S. (1981). *Three bureau of mines optical dust probes*. U.S. Bureau of Mines RI 8542.

Dahoe, A. E., Cant, R. S., Pegg, M. J., & Scarlett, B. (2001). On the transient flow in the 20-liter explosion sphere. *Journal of Loss Prevention in the Process Industries, 14*, 475–487.

Dorsett, H. G., Jr., Jacobson, M., Nagy, J., & Williams, R. P. (1960). *Laboratory equipment and test procedures for evaluating explosibility of dusts*. U.S. Bureau of Mines RI 5624.

Eckhoff, R. K. (1997). *Dust explosions in process industries*. Oxford: Butterworth-Heinemann, Ltd.

Eggleston, L. A., & Pryor, A. J. (1967). The limits of dust explosibility. *Fire Technology, 3*, 77–89.

Hertzberg, M., Cashdollar, K. L., & Opferman, J. J. (1979). *The flammability of coal dust–air mixtures*. U.S. Bureau of Mines RI 8360.

Hertzberg, M., Cashdollar, K. L., Zlochower, I. A., & Green, G. M. (1992). Explosives dust cloud combustion. In *Proceedings of the Twenty-fourth Symposium (International) on combustion* (pp. 1837–1843). Pittsburgh, PA: The Combustion Institute.

ISO 6184/1. (1985). *Explosion protection systems – Part 1: Determination of explosion indices of combustible dusts in air* (1st ed.). International Standardization Organization;

Kalejaiye, O.O. (2001). *An Investigation of the Effectiveness of Dust Dispersion in the Siwek 20-L Chamber*, Master of Applied Science thesis, Department of Chemical Engineering, Dalhousie University, Halifax, Nova Scotia, Canada.

Liebman, I., Conti, R., & Cashdollar, K. L. (1977). Dust cloud concentration probe. *Review of Scientific Instruments, 48*, 1314–1316.

Middleton, W. E. K. (1960). Bouger, Lambert, and the theory of horizontal visibility. *Isis, 51*, 145–149.

Montgomery, D. C., & Runger, G. C. (1999). *Applied statistics and probability for engineers*. New York: John Wiley & Sons, Inc.

National Fire Protection Association. (2002). *Guide for venting of deflagrations* (2002 ed.). Boston: NFPA 68.

National Instruments. (1994). *AT-MIO-16F-5 User Manual*.

Siwek, R. (1977). *20-l-Laborapparatur für die Bestimmung der Explosionskenngrossen brennbarer Staube*. [*20-liter laboratory apparatus for determination of explosion characteristics of combustible dusts*]. Winterthur, Switzerland: Ciba-Geigy AG (Basel) and Winterthur Engineering College.

Siwek, R. (1988). Reliable determination of the safety characteristics in 20-l apparatus. In *Proceedings of the Flammable Dust Explosion Conference* (pp. 529–573). St. Louis: Missouri.

Wells, L. K., & Travis, J. (1997). *LabVIEW for everyone*. New Jersey: Prentice Hall PTR.